

Design of 13.56 MHz Smartcard Stickers with Ferrite for Payment and Authentication

Michael Gebhart, Roland Neubauer, Michael Stark
NXP Semiconductors Austria GmbH Styria
Gratkorn, Austria
gebhart@ieee.org, {roland.neubauer, michael.stark}@nxp.com

Dimitri Warnez
NXP Semiconductors Germany GmbH
Hamburg, Germany
dimitri.warnez@nxp.com

Abstract—We present an adhesive sticker which allows contactless Smartcard function widely independent of the object material which it is stucked to. Recently interest raised for such a sticker to be attached on any mobile phone for contactless payment applications. This is seen as precursor of near field communication (NFC) technology helping to introduce contactless payment with mobile phone. In this context we consider antenna design with field simulation software and evaluate electrical antenna parameters of samples fabricated in the Smartcard process flow. Aspects for conformance to the ISO/IEC14443-2 and NFC card standard are considered and an optimized composite design is proposed.

I. INTRODUCTION

Over the last years the mobile phone has developed to a wireless personal multi-media information center, covering an increasing number of applications and being part of the standard equipment of practically every single person. Additionally, contactless Credit Cards are approaching mass market to supplement secure, microcontroller based applications. The combination of electronic payment and the mobile phone is a step further to end up in an all-in-one solution. The small form factor of some phones not only requires a reduction of size, compared to the Credit Card, but also different materials used for the phone case, plastic or metal, will severely degrade performance of conventional contactless technology. So this requires new antenna design concepts. As a first step, adhesive stickers with ferrite foil were developed to be attached on the back side of phones and operate autonomously, before they will be replaced by *Near Field Communication* (NFC) chips, directly integrated on the mobile phone printboard and having access to embedded Secure Elements (SE), Secure Device (SD) cards and Subscriber Identity Modules (SIM) in the phone. A similar example is a contactless module integrated in µSD cards, as proposed by companies like Tyfone [15], G&D [14] and Device Fidelity. However, further applications for such stickers are already coming up, e.g. secure authentication of sealed objects, which in principle have the same requirements as payment stickers to the contactless technology.

In this paper, we describe the design of 13.56 MHz loop antennas on ferrite material, to build up composite RFID Smartcard stickers operating nearly independent of any object material, which they are attached to.

II. PRINCIPLE OF OPERATION

Contactless transponder products in the 13.56 MHz range are powered by the *H*-field emission of a proximity reader. The magnetic flux of the alternating reader field passes through the turns of the resonant transponder loop antenna in free air and induces voltage. This is required for the Smartcard chip operation. In case the transponder is attached closely to a conductive metal case, the reader *H*-field generates eddy currents in this material, which cause a secondary *H*-field in phase opposition to the primary field. As a result, depending on the conductivity of the material, the magnetic flux through the loop antenna is nearly cancelled out. So the transponder is not powered, therefore the Smartcard function is prohibited.

To overcome this problem, ferrite material can be inserted between antenna loops and metal case. This material will conduct at least a part of the magnetic flux behind the transponder loop antenna. As a result, eddy currents originating from this part of the magnetic flux are prevented. This kind of *magnetic isolation* will allow the transponder to be powered at least by the part of the magnetic reader flux, which is conducted by the ferrite sheet.

The high relative permeability of the ferrite material close to the loop antenna will also affect electrical parameters of the equivalent antenna circuit and thus must be taken into account for proper design. The ferrite material will increase the antenna inductance. Moreover, there are additional losses in the ferrite material to be considered. This has drawbacks on resonance frequency and quality factor of the transponder.

In case there is conductive material present behind the sticker of such a design, the inductance is decreased. So there remains still an important dependency of this type of sticker. One option to reduce this dependency is to apply a metal layer (absorber) behind the ferrite. Such a composite design helps in two ways: first, the dependency on the phone case material is reduced a lot, so the Smartcard sticker is really “isolated”, and second, it also is shielded from unwanted emissions of a phone in plastic case, which at intermediate frequency (IF) level may be close to 13.56 MHz and could possibly have an impact on contactless Smartcard performance.

III. SMARTCARD ANTENNAS

A. Antenna design framework

Antennas for contactless near field systems in the 13.56 MHz frequency band are resonant loop antennas. The alternating (*active* and *reactive*) current in the antenna conductor is related to the alternating *H*-field in space as described by Maxwell's equations [1, 4].

Among the general conditions to start antenna design for cards, stickers or labels are typically:

- Requirements for the outline of the final product, referring to a *maximum size* for the antenna.
- The choice of one out of the four main antenna production technologies in this context, which are *wire embedding*, *etching*, *electroplating* in a galvanic process, or *printing* (e.g. silver ink or paste).
- The choice of chip package (e.g. module, or flip-chip).
- The choice of materials.
- The choice of an appropriate assembly process, e.g. *crimping*, *welding*, *soldering* or *conductive glueing*, and last but not least,
- an idea how the application should work, including ambient conditions (e.g. temperature, close coupling to metal or other objects) and standard requirements, to be interoperable with existing infrastructure. We consider these aspects in chapter IV.

For the actual antenna design there are two approaches: On the one hand analytical formulas, as we have described in previous work [7], allow estimations for simple structures, e.g. inductance of a rectangular coil, consisting of a circular wire conductor, which has little parasitic capacitance. Furthermore, this approach can easily take into account known process influences or allows estimations for changes in one parameter. On the other hand, there is computer aided design software (CAD) using the finite element method (FEM). We have used this approach to re-calculate our measurement results.

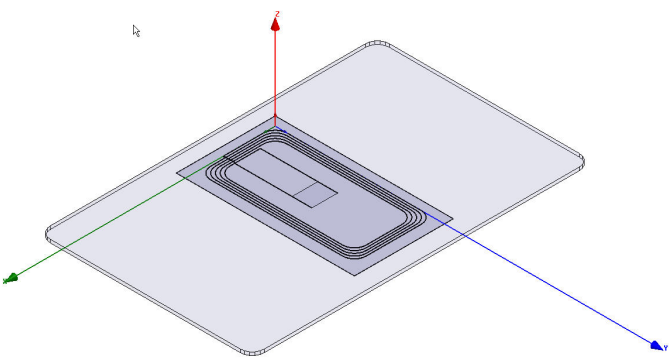


Fig. 1. Geometry for sticker on ferrite foil. 5 antenna designs of the same outline have been produced in the typical smartcard production flow.

The sticker product can be laminated in a card process, which allows to use already existing machines e.g. for personalization in the further process flow. The lamination process means to apply high temperature (e.g. 140 °C) and

pressure (e.g. 3.5 kN) over some time (e.g. 3 minutes) to bake the individual layers to one sheet body, of which the cards are punched out. Since the antenna wire is embedded in soft substrate material (e.g. polyvinyl chloride, PVC), the specified geometry may be changed in this process (e.g. shrink). The production of a series of coils with varied geometry is usually denoted as *antenna design matrix*. The antenna design matrix can be further used to fit an analytical model to the process.

In this study, we have used the analytical formula approach to estimate a series of antenna designs for ferrite stickers of a defined, limited size. A number of samples for each design has been produced with and without chip module assembled, to allow us characterization measurements. In a third step after measurement, the CAD field simulation software *High Frequency Structure Simulator* (HFSS) was used to simulate a design, to see how useful such a tool is in this context (in terms of the way how to model the structure, how accurately the results fit to measurements, and how much time and effort the calculation takes).

B. Antenna parameter measurement

Since the planar spiral loop antenna is a distributed element, like for all antennas, the complex impedance varies over frequency. For practical calculations, the electrical properties are represented in an equivalent circuit consisting of lumped elements. A simple parallel resonant circuit is sufficient to allow considerations for main aspects of high frequency HF transponder systems in Smartcard applications, although it is important to note this model is only valid precisely for *one frequency*.

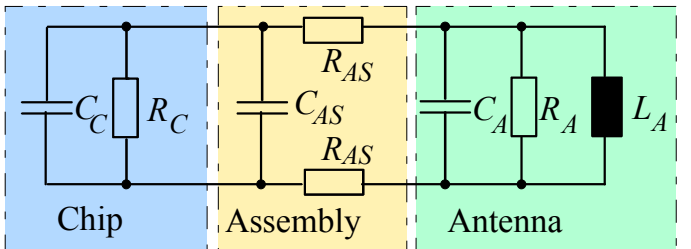


Fig. 2. Equivalent transponder circuit. Lumped elements represent the Smartcard chip (note that C_C and R_C are voltage dependent), the assembly connection of chip and antenna, and the loop antenna (note that C_A , R_A and L_A are frequency dependent).

The main electrical parameter of the antenna loop coil is the inductance L_A , consisting of some self-inductance due to coil length and mainly of mutual inductance due to coupling between the coil turns. In addition, there is also some parasitic capacitance C_A e.g. due to the electric coupling between the turns, and depending on the relative dielectric constant of the substrate material. In fact, this causes the reactive part of the impedance to change over frequency. Starting from inductive behaviour at low frequencies close to direct current (DC), the reactive impedance varies to a frequency where it becomes zero and which is defined as the self-resonance frequency f_S of the antenna, to a capacitive behaviour.

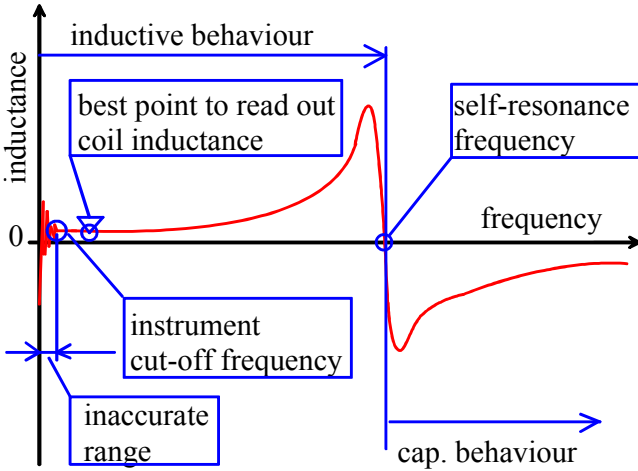


Fig. 3. Typical measurement trace of coil inductance over frequency.

The real part of the impedance is the resistance R_A , which consists of the frequency independent conductor resistance, and a frequency dependent component, consisting of the skin-effect and losses in the card substrate material.

The measurement of these parameters, e.g. using an Impedance / Network Analyzer or an LCR bridge, is done accordingly: Inductance is measured at a low frequency, but of course still well above the instrument cut-off frequency. 1 MHz is assumed to be a good choice for practice and was used in our measurements. The self-resonance frequency can be measured as the first point at which the complex impedance becomes real. Knowing the inductance, this allows to calculate C_A using the Thomson equation (1).

$$f_s = \frac{1}{2\pi\sqrt{L_A C_A}} \rightarrow C_A = \frac{1}{(2\pi f_s)^2 L_A} \quad (1)$$

The DC component of the resistance can be measured precisely close to DC with a Milliohm meter. Depending on the question, which frequency dependent losses we face in the antenna sample, the alternating current (AC) resistance can be measured in two ways: As first and more general option, it can directly be measured at the system carrier frequency f_C 13.56 MHz, where the antenna model is most interesting. This will be done, if there are several (even unknown) AC losses, e.g. in the card substrate or in the ferrite material. As second option, the parallel resistance can also be measured at the (higher) antenna self-resonance frequency f_s , and can then be calculated back to 13.56 MHz. This is more accurate, if AC losses are only caused by the skin effect, like for free air coils. Knowing that the resistance caused by skin effect is proportional to the square of the frequency, the equivalent parallel resistance at the operating frequency f_C can be calculated according to (2).

$$R_p(f_C) = \sqrt{\frac{f_s}{f_C}} R_p(f_s) \quad (2)$$

Knowing the equivalent inductance and resistance at f_C allows to calculate the Q-factor of the coil, according to (3).

$$Q_A(f_C) = \frac{R_A(f_C)}{2\pi f_C L_A} \quad (3)$$

For our considerations, a series of 5 embedded wire antenna designs with equal outline and varied pitch – the spacing between antenna turns – was produced on 200 μm PVC substrate and laminated with 2 x 50 μm ferrite foils of 45 x 25 mm size. The antenna parameters for an equivalent parallel resonant circuit, measured as described above, are given in table 1. For comparison the antennas were also measured as air coils on PVC substrate, with the ferrite sheets removed.

TABLE I
STICKER ANTENNA GEOMETRICAL AND ELECTRICAL PARAMETERS

| Antenna geometry data | | | | | |
|---|---------------|-------|-------|-------|---------|
| | outline | mm | No 1 | No 2 | No 3 |
| wire diam. | μm | | | | 40 x 20 |
| pitch | mm | 0.2 | 0.5 | 0.6 | 0.4 |
| turns | | 4 | 4 | 5 | 5 |
| Equivalent circuit electrical data for air coils on PVC | | | | | |
| L_A | μH | 1.595 | 1.304 | 1.692 | 1.937 |
| C_A | pF | 2.09 | 1.80 | 1.55 | 1.72 |
| R_A | k Ω | 16.97 | 12.40 | 17.92 | 21.81 |
| Equivalent circuit electrical data for coils on ferrite foils | | | | | |
| rel. perm. | μ_r | | | | 45 |
| thickness | μm | | | | 100 |
| L_A | μH | 2.008 | 1.649 | 2.162 | 2.433 |
| C_A | pF | 3.55 | 3.18 | 3.80 | 3.95 |
| R_A | k Ω | 12.85 | 10.18 | 11.91 | 13.80 |
| Relative increase of inductance due to ferrite sheet | | | | | |
| k_L | | 1.259 | 1.268 | 1.278 | 1.256 |
| | | 1.259 | 1.268 | 1.278 | 1.259 |

As can be seen in table 1, the inductance of the 5 designs varies in steps over a certain range, as it was the intention of the antenna design series. If we compare the inductance of the same designs with and without ferrite, we find the inductance is increased for the samples with ferrite foils, and moreover, inductance is increased by a similar factor k_L of about 1.26 for all designs. This can allow an estimation also for the inductance of stickers with ferrite, based on data for the air coil and this factor k_L , which closely depends on the product of relative permeability and thickness of the ferrite layer, according to investigations of TDK corporation. As another aspect we note a decrease in the antenna Q-factor Q_A for samples with ferrite layer, even though the inductance has increased. The reason are additional losses in the ferrite material at 13.56 MHz, which decrease R_A . As we show in chapter IV, these losses in the ferrite foil also have a negative impact on the transponder radio frequency (RF) performance.

C. Antenna simulation in HFSS

We have used the Ansoft HFSS field simulation software, version 11.2.1 to simulate sticker design 3 after the characterization measurements. This is a 3D full-wave electromagnetic field simulator which provides H - and E -fields, currents, near field and far field radiation patterns and can be used to calculate S-parameters. It allows to extract antenna inductance and capacitance in the same way, as described in section III B. Our intention was to estimate the effort (time) and the gain (accuracy) for this approach.

The generation of the geometric antenna model is the fundament for simulation. It is possible to import an existing CAD model, but we have choosen to build the structure based

on a library of existing bodies (e.g. box, cylinder, sphere) in the software. Variables were used for the dimensions of the model, e.g. wire diameter and pitch. Then, material properties have to be assigned to each created object. This can be selected from existing libraries, but we have chosen a manual definition (to have better control over parameters which are important for us). In our implementation, a user interface window allows to configure geometry and material for a specific design type.

Field simulation requires to define an adequate simulation volume, the *air box*. We have defined the surface of this air box to be *radiation boundary*, which allows waves to radiate infinitely into space. The distance between the outer faces of this volume to any radiating surface must be well chosen. On one hand it is related to the wavelength for the far-field limit which requires a large volume for low frequencies (such as 1 MHz), on the other hand it should be kept small to reduce simulation time. The antenna was centered in a 2 x 2 x 2 m air box for our simulation. Further, a second box of half the size of the outer air box was defined as *virtual object*. This approach optimizes accuracy and simulation time.

For the excitation of the antenna, a 50 Ohm port was defined, of same size and position as the chip module. As in the measurement, the antenna was simulated without chip. For the calculation of modal-based *S*-parameters the solution type *driven modal* was elected. A frequency range of 1 MHz – 100 MHz was simulated in steps of 10 kHz.

The convergence criteria are defined in the *solution setup*, for a *solution frequency* of 13.56 MHz. In addition to the convergence criterion for the maximum allowable change of *S* between two iterations (we selected 0.005) in the simulation run, a second criterion was defined for this antenna, which is the maximum change of the resistance (we selected 0.01). The resistance, however, will not fit accurately, as due to effort requirements we did not take the skin effect into account properly.

To decrease simulation duration some more refinements were made. The iterative solver was activated, the round wire circumference was belved to eight borders, mesh operations on the wire surface and inside the card were adapted and the size of elements of the initial mesh was defined to 0.15 times the wire diameter, to reduce complexity.

The results obtained from simulation are given in table 2.

TABLE II
SIMULATION RESULTS

| | <i>air coil</i> | <i>coil with ferrite foil</i> |
|--------------------|--------------------|-------------------------------|
| μ_r | 1 | 45 |
| L_A | 1.74 μH | 2.20 μH |
| C_A | 0.424 pF | 0.936 pF |
| k_L | --- | 1.264 |
| <i>Iterations</i> | 6 | 9 |
| <i>matrix size</i> | 648 703 | 1 866 303 |
| <i>Duration</i> | 2.78 h | 23.05 h |

A comparison to measurement results of table 1 shows a slightly increased absolute value for simulated inductance L_A (at 1 MHz). Interestingly, this applies for both, the air coil and the coil on ferrite, but the factor k_L again is 1.26. We interpret this rather as indication for a slight change of geometry during the fabrication process, as already mentioned in section III A, than as an inaccurate simulation result.

Regarding the effort, one run of the (prepared) simulation for the air coil took us 3 hours, with ferrite 23 hours. We have used a workstation with dual-core Intel Xenon processor 5110, 8 GB RAM and WXP 64 bit. This just gives an estimate, as during summer time we found, the simulation duration does not just correlate with complexity, but in practice also depends on environment conditions of the PC, especially temperature.

IV. RF SYSTEM CHARACTERISTICS

A successful communication with a contactless Smartcard system on the physical or RF Interface layer requires at least 3 aspects:

- The battery-less Smartcard transponder must be powered sufficiently by the reader alternating *H*-field.
- The transponder must be able to receive correctly the reader command.
- The reader must be able to receive correctly the transponder loadmodulation signal.

To guarantee interoperability, the base standard ISO/IEC14443 [18] in part 2 (RF Interface) defines limit values at the air interface, and the test standard ISO/IEC10373-6 [17] specifies the test bench and methods for measurement. For the Smartcard RF characteristics this refers to two parameters: The equivalent homogenous (averaged over the Calibration Coil area) minimum *H*-field required for operation (H_{min}), and the signal strength of the load modulation. We will focus on these two basic aspects and not consider others (which are also essential and specified in the standard), because they are most affected by the ferrite sheets.

A. Minimum *H*-field for operation

In a first measurement series we have built up a Smartcard sticker based on the NXP SmartMX P5CD081 [13] and design number 3, for one series as air coil on PVC card substrate and for a second series with 2 sheets of TDK IFL04 ferrite foil [11] below the coil and PVC, each 50 μm thick. A variable capacitor was connected in parallel to the chip, to be able to adjust the transponder resonance frequency in steps of 200 kHz around the energy optimum at the carrier frequency. The measurements were performed on an ISO/IEC10373-6 test bench as described in [2], and we have used a *REQUEST A* command to determine the limit for transponder operation. It should be noted, for applications like cryptographic operations as part of the payment application, the traces would be similar, but *H* increased due to a higher current consumption [6].

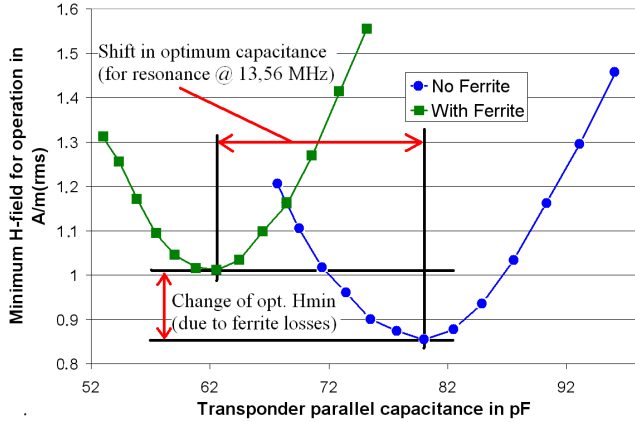


Fig. 4. Minimum H-field required for chip operation. The diagram shows 2 measurement series with varied capacitance; one for a sticker with ferrite foil, and one for an air coil sticker.

Fig. 4 shows two important aspects: As a first point, due to the antenna inductance change, the required capacitance to meet the optimum energy condition or the lowest H_{min} is significantly different. Seen from a different perspective, for a chip with a given integrated capacitance (average value +/- tolerances), there will be a significant *decrease* in transponder resonance frequency if an air coil is laminated above a ferrite foil. In this case, the frequency shift is 1.7 MHz for a 70 pF chip input capacitance. And although both traces are similar, we can observe as second point, the H_{min} value achieved with the ferrite design is *increased* over the value achieved with the air coil. The main root causes for this behaviour are losses in the ferrite foil, which depend on the material characteristics, e.g. conductance, as given in the data sheet [11]. A second root cause is the difference in the relation between L_A and C_A , which affects the transponder Q -factor Q_T at the start of operation point, as explained in [7]. Thus we cannot perfectly compare the two traces.

B. Load Modulation

The second base aspect is load modulation. We have used the same Smartcard stickers of design number 3. For this measurement, both transponders were adjusted to 13.56 MHz resonance frequency at their start of operation voltage (with different values for the parallel capacitors). The same testbench was used as in the previous section [2], but it is important to note we have already used the new introduced PCD 2 antenna arrangement for small transponder antenna classes 4 – 6 [16]. In fig. 5 we compare the load modulation level (phasor) of the upper side band at 14.4075 MHz according to the ISO/IEC10373-6 test method.

In addition to the increase of H_{min} for the sample with ferrite foil compared to the free air coil transponder we can observe a decrease of the load modulation of about 4 mV in the voltage limited region (> 3 A/m for both antennas), which is a reduction of about 15 %.

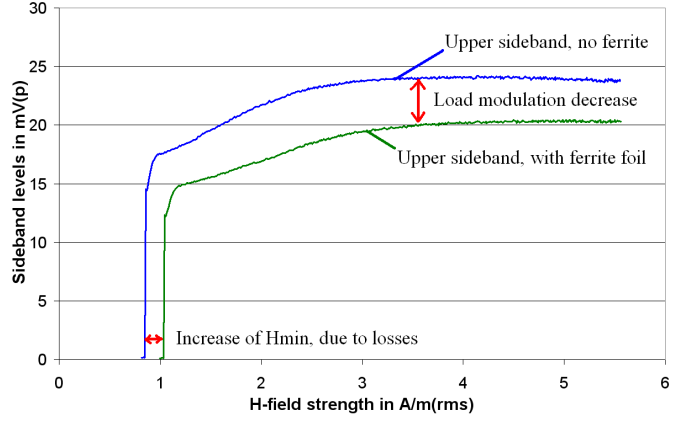


Fig. 5. Upper sideband (14.4075 MHz) level of sticker load modulation. The diagram compares a sticker of design number 3 with and without ferrite foil. A decrease of about 15 % of the load modulation level can be observed.

V. COMPOSITE STICKER DESIGN

For the Smartcard sticker considered so far, we have found an increase of the required H -field for chip operation and a decrease of the load modulation. Both applies if the transponder is operated at the energy-optimum resonance frequency, which is equal to the carrier frequency. However, in the application it is not known, if the transponder is stucked on metal or plastic material. The inductance of a coil is increased in close coupling to ferrite material, but it is decreased (and accordingly the resonance frequency is increased) for coupling to metal, as shown by Qing et al. [5]. So for the sticker design presented in table 1 this wide range of resonance frequencies is the main drawback. It is constituted not only from production tolerances but mainly from the application. To provide Smartcard functionality based on reliable RF characteristics means that we have to reduce tolerances, to allow a design for *one* optimum resonance frequency. Thus, the goal is to isolate the transponder from ambient influence as good as possible. An option here is to integrate a metal foil layer below the ferrite layer in a composite sticker, and to take this into account for antenna design. The design concept is shown in fig. 6.

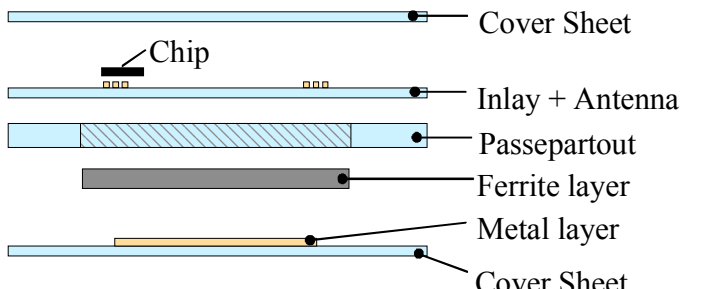


Fig. 6. Composite design for a magnetically "isolated" contactless Smartcard.

For optimum performance we found, that the ferrite layer outline should be *larger* than the coil outline, to allow the

magnetic flux to turn around the current in the coil windings. For an antenna size as considered here, 2.5 mm is a good choice. On the other hand, the metal layer area should be *smaller* than the coil outline.

With such a design we could reduce the maximum resonance frequency shift to about 0.2 – 0.3 MHz, which seems tolerable. Additionally, the metal foil helps to shield possible *E*-field emissions from the phone, for plastic cases.

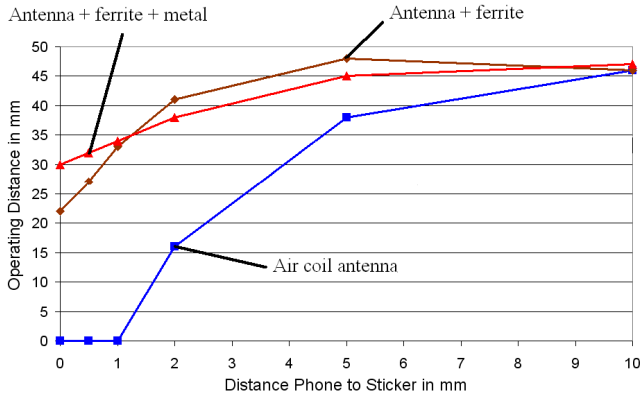


Fig. 7. Operating distance for Smartcard stickers of different designs on EMVCo 2.0 test bench. The diagram compares RF performance of antenna concepts as discussed in this work.

An illustrative RF performance comparison for 3 approaches: Air coil, air coil on ferrite foil, and composite design, is shown in fig. 7. We have mounted a metal plate of 100 x 70 x 1 mm in varied distance of 0 – 10 mm behind the (centered) Smartcard stickers, to emulate the scenario of an adhesive sticker on a metal phone case. For this measurement we have used the EMVCo 2.0 testbench [20]. This test bench is used for product certification of contactless payment. For *nominal field* conditions we have noted the maximum achievable distance for Smartcard operation (our criterion was an observable response to the *REQUEST A* command).

No communication distance was achievable with the air coil mounted 0 – 1 mm distance to the metal plate. Some distance (e.g. 22 mm) was achievable with ferrite foil, more (e.g. 30 mm) with the composite design. This is here the practical use case. The air coil communication distance increases with distance to the metal plate, and at 10 mm is already equal to the more sophisticated designs. Note, a distance of 10 mm is a rather unrealistic scenario and thus of theoretical nature.

VI. CONCLUSION

We have discussed antenna design options to allow contactless Smartcard operation on all materials. A ferrite foil behind the antenna can be used for well determined ambient conditions (e.g. operation on a metal phone case). For a practical design example we have compared measured equivalent antenna parameters of fabricated samples with field simulation results. As we found, the *absolute value of simulated inductance* was slightly different to measurements, for the air coil as well as for the design on ferrite foil. This was explained by geometry changes in the fabrication process. However, the simulation of *relative change k_L* due to the

ferrite foil fits very well to measurement results. We have shown the quantitative performance degradation for this design, about 15 % increase of *Hmin* and 15 % decrease of load modulation. For unknown ambient conditions we have proposed an efficient composite design to magnetically *isolate* the Smartcard. This design reduces the wide range of resonance frequencies to be taken into account for different ambient coupling conditions, which is essential to achieve reliable contactless performance.

REFERENCES

- [1] J. C. Maxwell, *A Treatise on Electricity and Magnetism*, 3rd ed., Vol.2., Oxford: Clarendon, 1892.
- [2] M. Gebhart, S. Birnstingl, J. Bruckbauer, E. Merlin, "Properties of a test bench to verify Standard Compliance of Proximity Transponders", in CSNDSP, July 2008, pp. 306-310.
- [3] T. Simpson, "Electrically Small Spheroidal Loops Wound on Hollow Ferrite Cores", in *IEEE Antennas and Propagation Magazine*, Vol. 50, No. 3, June 2008.
- [4] H. A. Wheeler, "Fundamental Limitations of Small Antennas", Proc. I.R.E., December 1947, pp. 1479–1484.
- [5] X. Qing, Z. N. Chen, "Proximity Effects of Metallic Environments on High Frequency RFID Reader Antenna: Study and Applications", in *IEEE Transactions on Antennas and Propagation*, Vol. 55, No. 11, November 2007.
- [6] M. Gebhart, J. Bruckbauer, M. Gossar, "Chip Impedance Characterization for Contactless Proximity Personal Cards", in CSNDSP, July 2010, pp. 826–830.
- [7] M. Gebhart, R. Szoncsó, "Optimizing Design of Smaller Antennas for Proximity Transponders", in 2nd International Workshop on NFC, April 2010, pp. 77–82.
- [8] B. Y. Tsirline, "Spatially Selective Antenna for Very Close Proximity HF RFID Applications", in *High Frequency Electronics*, February 2007, pp. 18–28.
- [9] M. Baum, B. Niemann, F. Albeck, D. H. Fricke, "Qualification Test of HF RFID Foil Transponders for a Vehicle Guidance System", in ITSC 2007, pp. 950–955.
- [10] H. Zhu, S. Lai, H. Dai, "Solutions of Metal Surface Effect for HF RFID Systems", in WiCom 2007, ISBN 978-1-4244-1311-9, pp. 2089–2092.
- [11] TDK corporation, *TDK Flexield*, data sheet, 2009 (www.tdk.co.jp/absorber/).
- [12] S.-G. Pan et al., "Design of loop antennas and matching networks for low-noise RF receivers: Analytic formula approach", in IEE Proc. on Microwaves, Antennas and Propagation, Vol. 144, Issue 4, August 1997, pp. 274–280.
- [13] NXP Semiconductors, P5CD016/021/041 and P5Cx081 family, Product data sheet, Rev. 3.0, 3 July 2009.
- [14] W. Rankl, W. Effing, *Smart Card Handbook*, Wiley & Sons, 4th edition, 2010.
- [15] S. G. Narendra, A. Chandrakasan, *Leakage in Nanometer CMOS Technologies*, Springer Publications, 2006, ISBN 0-387-25737-3.
- [16] ISO/IEC 10373-6:2001/FPDAM 8.3, *Identification cards – Test methods – Part 6: Proximity cards. Amendment 8: Additional PICC classes*, ISO/IEC JTC 1/SC 17/WG 8, N1740, 2010-10-07.
- [17] ISO/IEC 10373-6:2010, *Identification cards – Test methods – Part 6: Proximity cards*.
- [18] ISO/IEC FDIS 14443-2:2009(E), *Identification cards – Contactless integrated circuit(s) cards – Proximity cards – Part 2: Radio frequency power and signal interface*, ISO/IEC JTC 1/SC 17/WG 8, N1512, 2009-07-26, (www.wg8.de).
- [19] T. Bauernfeind, K. Preis, O. Biro, G. Koczka, F. Hämmeler, "Calculation of equivalent circuit parameters for a high frequency RFID transponder", Proc. of the 17th Conf. on the computation of electromagnetic fields, November 2009, pp. 883 – 884.
- [20] EMV *Contactless Specifications for Payment Systems*, Version 2.0.1, July 2009 (www.emvco.com/specifications.aspx?id=21).